2012

Atmospheric validation of high accuracy CO2 absorption coefficients for the OCO-2 mission

David R. Thompson

Linda R. Brown

David Crisp

D. Chris Benner
William & Mary, dcbenn@wm.edu

V. Malathy Devi
William & Mary, mdvenk@wm.edu

Recommended Citation

Thompson, David R.; Brown, Linda R.; Crisp, David; Benner, D. Chris; and Devi, V. Malathy, Atmospheric validation of high accuracy CO2 absorption coefficients for the OCO-2 mission (2012). *Journal of Quantitative Spectroscopy & Radiative Transfer*, 113(17), 2265-2276.
10.1016/j.jqsrt.2012.05.021

Journal of Quantitative Spectroscopy & Radiative Transfer 113 (2012) 2265–2276

Contents lists available at SciVerse ScienceDirect

Journal of Quantitative Spectroscopy & Radiative Transfer

journal homepage: www.elsevier.com/locate/jqsrt

Atmospheric validation of high accuracy CO_2 absorption coefficients for the OCO-2 mission

David R. Thompson [a,*], D. Chris Benner [b], Linda R. Brown [a], David Crisp [a], V. Malathy Devi [b], Yibo Jiang [a], Vijay Natraj [a], Fabiano Oyafuso [a], Keeyoon Sung [a], Debra Wunch [c], Rebecca Castaño [a], Charles E. Miller [a]

[a] Jet Propulsion Laboratory, California Institute of Technology, 4800 Oak Grove Dr. Pasadena, CA 91109, USA
[b] Department of Physics, The College of William and Mary, Box 8795, Williamsburg, VA 23187, USA
[c] California Institute of Technology, 1200 East California Boulevard, Pasadena, CA 91125, USA

ARTICLE INFO

Article history:
Received 13 March 2012
Received in revised form
25 May 2012
Accepted 29 May 2012
Available online 12 June 2012

Keywords:
Fourier transform spectroscopy
Infrared CO_2 spectroscopy
Atmospheric CO_2 retrievals
Line shapes
Line mixing
Speed dependence

ABSTRACT

We describe atmospheric validation of 1.61 μm and 2.06 μm CO_2 absorption coefficient databases for use by the Orbiting Carbon Observatory (OCO-2). The OCO-2 mission will collect the measurements needed to estimate column-averaged CO_2 dry air mole fraction within 1 ppm accuracy without the region- or airmass-dependent biases that would significantly degrade efforts to understand carbon sources and sinks on a global scale. To accomplish this, the forward radiative transfer model used to generate synthetic atmospheric spectra for retrievals must achieve unprecedented spectroscopic fidelity within the short wave infrared CO_2 bands sampled by the sensors. The failure of Voigt line shapes and conventional line mixing formulations for such objectives has motivated significant revisions to line shape models used to generate the gas absorption cross sections for the OCO-2 forward model. In this paper, we test line mixing and speed dependent line shapes combined with improved experimental line parameters. We evaluate pre-computed absorption coefficients in the two spectral regions of CO_2 absorbtion using high resolution FT-IR laboratory spectra, atmospheric spectra from the Total Carbon Column Observing Network (TCCON), and medium resolution soundings from the space-based Greenhouse Gases Observing Satellite (GOSAT).

1. Introduction

Our current understanding of the atmospheric carbon cycle relies mainly on combining CO_2 measurements from ground sensor networks with transport models to inform flux inversions [1–3]. Space-based measurements of CO_2 can make significant contributions by observing areas that ground-based instruments cannot access, such as the open ocean or deep rain forest. More importantly, high precision data can expand the spatial and temporal coverage to reveal regional sources and sinks [3–7]. This will be critical for assessing the extent and variability of these fluxes as well as their sensitivity to future climate change.

Recent advances in space based remote sensing observations of CO_2 and other greenhouse gases hold promise for global monitoring efforts [8–12]. Measurements of the absorption of reflected sunlight by CO_2 can provide estimates of the column averaged CO_2 dry air mole fraction, $\mathbf{X}_{CO2}$, which are sensitive to CO_2 variations near the surface where most sources and sinks are located. The Japanese Greenhouse gases Observing SATellite (GOSAT) and the NASA Orbiting Carbon Observatory (OCO) were the first two satellites specifically designed to exploit this approach. GOSAT was successfully launched in January

* Corresponding author. +1 818 354 2200.
E-mail address: david.r.thompson@jpl.nasa.gov (D.R. Thompson).

0022-4073/$ - see front matter © 2012 Elsevier Ltd. All rights reserved.
http://dx.doi.org/10.1016/j.jqsrt.2012.05.021

2009 and has been routinely collecting CO_2 and methane observations over the sunlit hemisphere of the globe since April 2009 [13–15]. OCO was lost in February 2009 when its launch vehicle malfunctioned and failed to reach orbit. A replacement called OCO-2 is currently under development in preparation for a late 2014 launch.

Precise $\mathbf{X}_{CO2}$ measurements are needed because surface sources and sinks of CO_2 produce small spatial and temporal variations in this quantity [4]. While the atmospheric CO_2 mixing ratio can vary by as much as 8% near the ground, these perturbations decay rapidly with height such that $\mathbf{X}_{CO2}$ variations rarely exceed 2% on regional scales. Existing data show that $\mathbf{X}_{CO2}$ variations are usually no larger than 0.3% on regional scales, and that these variations have representative spatial scales that range from 100 km over continents to 1000 km over the ocean. Resolving the most important regional fluxes necessitates accuracy to within 0.25% (1 ppm) [4].

To meet these precision requirements, the GOSAT and OCO-2 instruments acquire high resolution spectra in three spectral ranges: two for estimating CO_2 abundance using rovibrational absorption bands at 1.61 μm and 2.06 μm, and one for simultaneous measurement of the O_2 A band at 0.76 μm to determine photon path length and surface pressure [16]. The OCO-2 retrieval algorithm [16,17] uses a forward radiative transfer model to simulate an observed spectrum for a given atmospheric state. An inverse model, based on optimal estimation [17], then uses the differences between the observed and simulated spectrum to modify the state properties and improve the fit [8–10]. Because a 0.25% variation in the CO_2 column abundance produces spectral variations that are much smaller than this, both high precision measurements and a high fidelity forward model are needed. The forward model must account for all physical phenomena that contribute to the atmospheric spectrum such as absorption, gas and aerosol scattering, surface reflectance, surface pressure, and the atmospheric temperature and water vapor profiles [12,16].

Only a small fraction of the uncertainty budget remains for uncertainties in CO_2 and O_2 spectroscopy [4,18]. Consequently evaluation and refinement of the retrieval spectroscopic models has been an important part of the OCO-2 preparatory effort. To validate the spectroscopic molecular line parameters used in the forward model, we must demonstrate a radiometric accuracy of 0.1% on laboratory spectra which approaches the peak-to-peak errors of the best fits. Systematic errors are of particular concern since they introduce regional biases that imitate sources and sinks [4,19].

This paper focuses on the pressing challenge of CO_2 absorption at 1.61 μm and 2.06 μm. Ground-based studies report inconsistencies in the CO_2 total columns retrieved using these two spectral regions and attribute systematic errors to the basic line parameters (such as line intensities and Voigt pressure broadening coefficients) [12,16,20,21]. At the same time, laboratory studies demonstrate that the choice of molecular line shape impacts the retrieved line parameters. In addition to Lorentz broadening, one must consider the combined effects of Line Mixing (LM), speed dependence and narrowing [18,22–24]. The best line shape choice is still uncertain, but profiles which model line mixing and speed dependence provide superior fits to CO_2 lab data [23] while line mixing improves atmospheric retrievals [25]. Non-Voigt line shapes also provide more physically plausible values for related line parameters [24].

Several groups have used new LM models for infrared remote sensing of CO_2. LM was introduced into the Atmospheric Infrared Sounder (AIRS) retrieval algorithm for 14 μm spectral soundings [26], and demonstrated in Fourier Transform Spectrometers on balloon and aircraft platforms [27]. New LM models have significantly improved fits to upward-looking atmospheric spectra in the OCO-2 bands [28,29]. However the best fits still show persistent structured residuals at 2.06 μm [25]. Speed dependent line shapes remain virtually unused in atmospheric retrievals due to their computational complexity and the lack of standardized software, atmospheric, and laboratory evaluation benchmarks. Some combination of the non-Voigt line shapes is needed to achieve the radiometric accuracy required for OCO-2.

This work describes the first atmospheric tests of CO_2 absorption cross sections derived from new laboratory studies that combine LM parameters [30] with a speed dependent line shape profile [31–33]. First we apply the proposed database to high-resolution laboratory spectra acquired under homogeneous conditions with controlled gas abundances, temperature, and illumination. We then perform atmospheric retrievals of $\mathbf{X}_{CO_2}$ with solar observations from the Total Carbon Column Observing Network (TCCON) [20,21,34]. These upward-looking spectra are a conceptual bridge between the laboratory and orbital retrieval scenarios. They are simpler than the downward-looking case due to improved SNR, the lack of significant optical path length biases associated with scattering, and direct sensing of atmospheric conditions at the surface. The path lengths reveal weak CO_2 lines to a degree unattainable under typical laboratory conditions, providing an independent validation of the new line parameters. Finally, we test orbital soundings using the OCO-2 retrieval algorithm. We consider a representative set of GOSAT orbits with hundreds of soundings acquired by the TANSO-FTS instrument [12]. The GOSAT tests use the full OCO-2 Level 2 retrieval algorithm and the associated challenges of aerosol scattering, surface reflectance, and lower SNR [16]. These demonstrate non-Voigt line shapes in an atmospheric retrieval process capable of meeting strict throughput requirements for OCO-2, which is expected to yield approximately 10^5 cloud-free soundings each day.

2. Absorption coefficient models

The new cross sections are based on a multispectrum parameter fitting procedure that combines dozens of laboratory spectra in a least-squares optimization. Low pressure spectra provide intensities and line positions, while higher pressure scans characterize line mixing, self- and air-broadened half widths. We refer the interested reader to a description by Benner et al. [35] and supporting texts by Vitcu [33] and Predoi-Cross et al. [31]. We will review the most important aspects here.

2.1. Line Mixing

Line Mixing (LM) is a broad topic for which Hartmann et al. provide a comprehensive review [36]. Our specific formulation follows Predoi-Cross et al. and Levy et al. [37,38]. We express the combined absorption from a spectrum of interacting Lorentz lines as a function $I(\omega)$ of frequency ω:

$$I(\omega)=\frac{1}{\pi}\mathrm{Im}[\mathbf{X}^T(\mathbf{1}\omega-\omega_0-iW)^{-1}\rho\mathbf{X}] \quad \text{for } \mathbf{X}_j=\sqrt{S_j/\rho_j} \tag{1}$$

Here $\mathbf{1}$ is the identity matrix and ω_0 is a diagonal matrix of zero-pressure line positions. The diagonal matrix ρ holds relative populations for lower energy states, and $\boldsymbol{X}$ is a vector with an element for each line j given by intensity S_j and the number density ρ_j. The *relaxation matrix* W determines the strength of coupling between interacting pairs of lines [36]. Diagonal elements of W have real and imaginary parts representing Lorentz half widths α_L and pressure shifts δ:

$$W_{jj}=\alpha_{Lj}-i\delta_j \tag{2}$$

Off-diagonal elements describe mixing between different transitions. These are proportional to pressure, and have the same units as the Lorentz half width. We compute a matrix element W_{jk} by summing contributions W_{jkr} for each broadening gas r in proportion to volume mixing ratio χ_r:

$$W_{jk}=\sum_r \chi_r W_{jkr}(T_0)\left(\frac{T_0}{T}\right)^{m_{jkr}} \tag{3}$$

Temperature dependence exponents m are relative to a reference temperature T_0 (296 K). The off-diagonal relaxation matrix elements satisfy a *detailed balance* relationship:

$$W_{kj}=\sum_r \chi_r\left(\frac{\rho_{kr}}{\rho_{jr}}\right)W_{jkr}(T_0)\left(\frac{T_0}{T}\right)^{m_{jkr}} \tag{4}$$

These elements are interdependent with Lorentz widths and pressure shifts, so it is important to retrieve all parameters simultaneously.

Evaluating Eq. (1) requires a matrix inversion for each spectral point. Following Pine [39], we transform Eq. (1) into a more convenient representation using *generalized line parameters* [39]. We diagonalize the matrix ω_0+iW using:

$$A^{-1}(\omega_0+iW)A=\Lambda \tag{5}$$

The columns of A are normalized eigenvectors whose eigenvalues correspond to entries in the diagonal matrix Λ. We further define:

$$\xi_j=\mathrm{Re}[(X^TA)_j(A^{-1}\rho X)_j] \tag{6}$$

$$\eta_j=\mathrm{Im}[(X^TA)_j(A^{-1}\rho X)_j] \tag{7}$$

Eq. (1) is then equivalent to the following expression [38,39]:

$$I(\omega)=\frac{1}{\pi}\sum_{j=1}^{N}\frac{\xi_j\mathrm{Im}[\Lambda_{jj}]+\eta_j(\omega-\mathrm{Re}[\Lambda_{jj}])}{\mathrm{Im}[\Lambda_{jj}]^2+(\omega-\mathrm{Re}[\Lambda_{jj}])^2} \tag{8}$$

This has the same form as a Rosenkranz first-order LM approximation:

$$I_R(\omega)=\frac{1}{\pi}\sum_{j=1}^{N}S_j\left[\frac{\alpha_{L_j}+Y(\omega-\omega_{0j})}{\alpha_{L_j}^2+(\omega-\omega_{0j})^2}\right] \tag{9}$$

Consequently we can evaluate Eq. (1) using a sum of Lorentz profiles with first-order line mixing. These "pseudo-profiles" use the following generalized parameters: the intensity S_j becomes ξ_j, the first order line mixing parameter Y times the line intensity S_j becomes η_j, the line spectral position ω_{0j} becomes $\mathrm{Re}[\Lambda_{jj}]$, and the Lorentz half width α_{L_j} becomes $\mathrm{Im}[\Lambda_{jj}]$. The resulting absorption cross sections are mathematically equivalent to the complete spectrum of mixed Lorentz lines [39]. In principle, many lines are coupled and the magnitude of the mixing effect decreases smoothly with increasing separation [40]. In practice the limited number of laboratory spectra do not provide enough constraints to fit all the terms in the full relaxation matrix W. Instead, we desire a constrained parameterization with appropriate flexibility for our atmospheric application. The OCO-2 approach fits all tridiagonal matrix terms, explicitly modeling interaction between neighbor lines of P- and R-branches [30]. The tridiagonal relaxation matrix uses immediate neighbor coefficients to approximate the influence of the more distant lines. The carbon dioxide lines in these bands are spaced widely enough that the approximation is effective for atmospheric pressures and temperatures. We set these parameters directly with simultaneous fits of multiple lab spectra, holding all other off-diagonal relaxation matrix elements to zero [23,30].

2.2. Speed dependent line shapes

Here we extend Eq. (8), which describes a mixed Lorentz profile, to incorporate Doppler broadening and speed dependence effects. A speed dependent profile [31,32] refines the Lorentz contribution by accounting for various speeds at the time of collision. Specifically, it is the convolution of Doppler and Lorentz profiles integrated over possible collision speeds. While there is no consensus on the best physical model or line shape for NIR CO_2 spectra, profiles using a quadratic speed dependence have been shown to fit laboratory data better than a standard Voigt model [24]. One can compute a speed dependent line shape using a combination of two Voigt profiles [32] or, as in this work, by numerical integration. We employ a quadratic speed dependence relationship first introduced in [41], detailed in Vitcu [33] and further elaborated by Benner et al. [30]. Like the complex Voigt profile, the speed dependent Voigt $V_s(\omega)$ has real and imaginary parts:

$$V_s(\omega)=K_s(\omega)+iL_s(\omega) \tag{10}$$

We parameterize each collisionally isolated line, j, using the Lorentz half width, α_{Lj}, spectral line position, ω_{0j}, a speed dependence parameter, s_j, and a Dicke narrowing parameter, H_j. Convolving Lorentz and Doppler profiles and integrating over velocity [42], we have

$$K_s(\omega)=\frac{2}{\pi}\int_{-\infty}^{\infty}ve^{-v^2}\tan^{-1}(Q_s(v,\omega))\,dv \tag{11}$$

$$L_s(\omega) = \frac{1}{\pi}\int_{-\infty}^{\infty} \nu e^{-\nu^2} \ln(1+Q_s(\nu,\omega)^2)\, d\nu \quad (12)$$

where α_D is the Doppler half width and $Q_s(\nu,\omega)$ is given by

$$Q_s(\nu,\omega) = \frac{\omega-\omega_{0j}+\nu\alpha_D}{\alpha_{Lj}[1+s_j(\nu^2-1.5)]+H_j} \quad (13)$$

We substitute the generalized Lorentz line parameters defined in Section 2.1 into this expression in order to capture the combined effects of speed dependence, Doppler broadening and line mixing.

In this work the Dicke narrowing parameter H_j is always set to zero because narrowing and speed dependence can both alter the line shape in similar ways, and distinguishing the two effects requires very high spectral resolution. In the laboratory data the CO_2 Doppler width is close to the FTS Instrument Line Shape. Consequently, in the spectra where Dicke narrowing is most active, each narrow line provides a single point measurement with only enough information to retrieve position and intensity. Other ways to estimate Dicke narrowing include computing H_j directly from the gas diffusion constant or retrieving it from measurements with higher spectral resolution.

2.3. Continuum effects

Apart from LM effects, previous researchers have raised the possibility that Collision Induced Absorption (CIA) could play a role in NIR rovibrational transitions for CO_2 [25]. Recent results by Lamouroux et al. [28] provide an upper limit on CIA for NIR CO_2 that would be negligible in the atmosphere [28]. Our basic parameterization does not include CIA, but continuum-level effects may still arise in atmosphere due to solar lines or unmodeled atmospheric absorption. We found that we could improve atmospheric retrieval performance with a small *ad hoc* continuum absorption. We generate the pressure continuum with a pair of Gaussian distributions centered at 4853.5 and 4789 cm^{-1}, with respective widths 10 and 8 cm^{-1} and peak intensities of 2.1×10^{-24} and 4.2×10^{-25} cm^{-1}/(molecule cm^{-2}). These parameters were determined by empirical modification to improve fits to atmospheric spectra. This modification is directly proportional to pressure, though a "pressure squared" correction yields similar results. In general, atmospheric tests do not yet provide strong evidence to show if this is caused by physical atmospheric effects, modeling error, or a computational artifact.

2.4. Table computation

The OCO-2 mission will produce approximately 10^5 cloud-free soundings per day. To satisfy retrieval data throughput requirements we perform all cross section computations in advance. This is particularly important for computationally intensive LM calculations having many pairwise interactions between lines. We cache the absorption coefficients in a lookup table (ABSCO table) indexed by pressure and temperature. The tests that follow use a spectral grid spacing of 0.002 cm^{-1}. We record cross sections at 70 pressures evenly spaced at 1 kilometer altitude increments. The 17 temperature levels lie on an evenly spaced grid centered at the mean vertical temperature profile for historical GOSAT retrieval footprints, as given by the European Centre for Medium-Range Weather Forecasts (ECMWF). This provides coverage over all physically reasonable atmospheric conditions. At runtime, a linear interpolation provides cross sections.

Table 1 summarizes our spectroscopic data sources for the proposed databases. A modified version of the multispectrum nonlinear least squares fitting technique of Benner et al. [30] computes the main isotopologue for CO_2 lines near 4850 and 6200 cm^{-1} using a speed dependent line profile. As mentioned previously, these parameters originate from a least squares multispectrum retrieval process described in [35] with laboratory results reported in [23,30].

Fig. 1 shows a typical fit of the 2.06 μm CO_2 band to a laboratory spectrum from the JPL Bruker FTS instrument [46]. Here, a low pressure HCl cell in line with the main cell was used to characterize the instrumental line shape and provide an absolute frequency calibration. This spectrum contributed to the multispectrum fitting procedure. The subsequent cross section tables reproduce a good quality fit, which provides confidence in the calculation. Peak residuals near 0.1% may be related to line shape, and approach the limits of laboratory accuracies achievable with this parameterization. The residuals are expressed in terms of the maximum transmission level. The right panel gives an expanded view of the residual structure near 4824.5 cm^{-1}. Fig. 2 shows a 1.61 μm spectrum not incorporated into the Devi et al. fits [23]. This is a more challenging case, since transmittance is computed without modifying line parameters to fit the experimental data. Only the volume mixing ratio is optimized, and it converges to a value within 2% of the recorded estimate. Peak residuals are a small fraction of a percent, and the retrieved CO_2 volume mixing ratio is within the uncertainty in laboratory conditions.

3. Atmospheric evaluation and results

3.1. The TCCON uplooking FTS network

TCCON is a global network of upward-looking FTS spectrometers that measures transmittance along a direct

Table 1
Parameter sources for the proposed CO_2 spectroscopic line list. Note: only first authors are shown.

Parameter	**2.06** μm CO	**1.61** μm CO
Positions	Benner [30]	Devi [23]
Intensities	Benner [30]	Devi [23]
Air-widths	Benner [30]	Predoi-Cross [43]
Air-shifts	Benner [30]	Predoi [43], Devi [23]
Air-width T dependence	Benner [30] from Predoi [43]	Predoi[43]
Line shapes	SD+LM	SD+LM
Isotopologues	Toth [44], Rothman [45] (text)	Rothman [45] (text)
Air LM	Benner [30]	Devi [23]
Speed dependence	Benner [30]	Devi [23]
Continuum	n/a	(See text)
Collisional narrowing	n/a	n/a

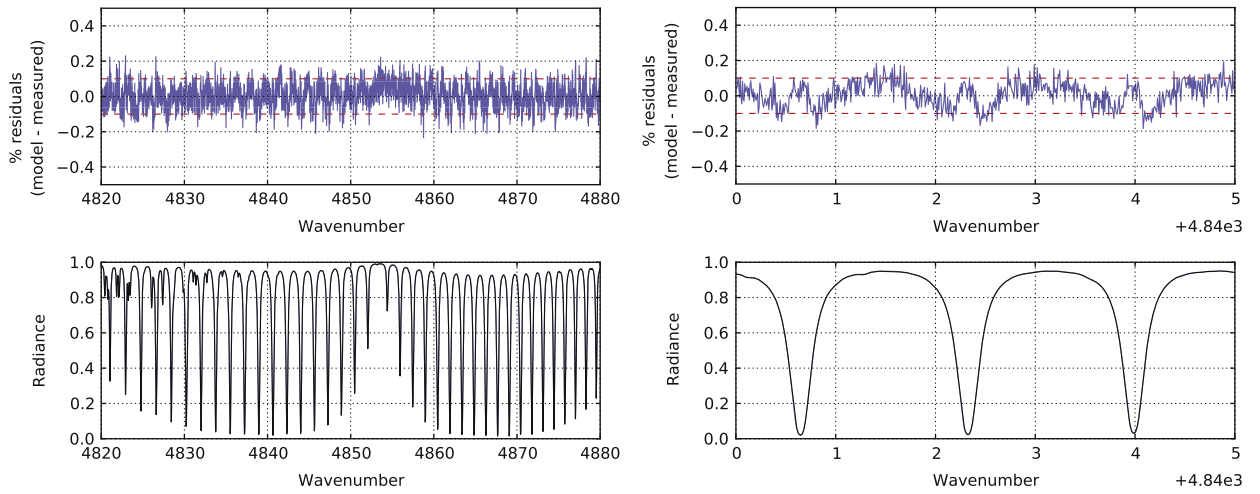

Fig. 1. Modeling an air-broadened CO_2 laboratory spectrum at 2.06 μm (wavenumber=cm^{-1}) by applying line parameters for a speed dependent profile with line mixing from [30]. The upper panel shows the residuals obtained for the scan in the lower panel. The plot at right is an expanded view for a spectral range centered at 4842.5 cm^{-1}, and the red dashed lines mark the 0.1% radiometric accuracy target. The lab spectrum was recorded at 0.00444 cm^{-1} resolution (optical path difference 112.5 cm) using a multipass absorption cell set at 29.30 m optical path length. The total gas pressure was 599.8 Torr at 296.1 K with 4.95% being ^{12}C-enriched $^{16}O^{12}C^{16}O$. (For interpretation of the references to color in this figure caption, the reader is referred to the web version of this article.)

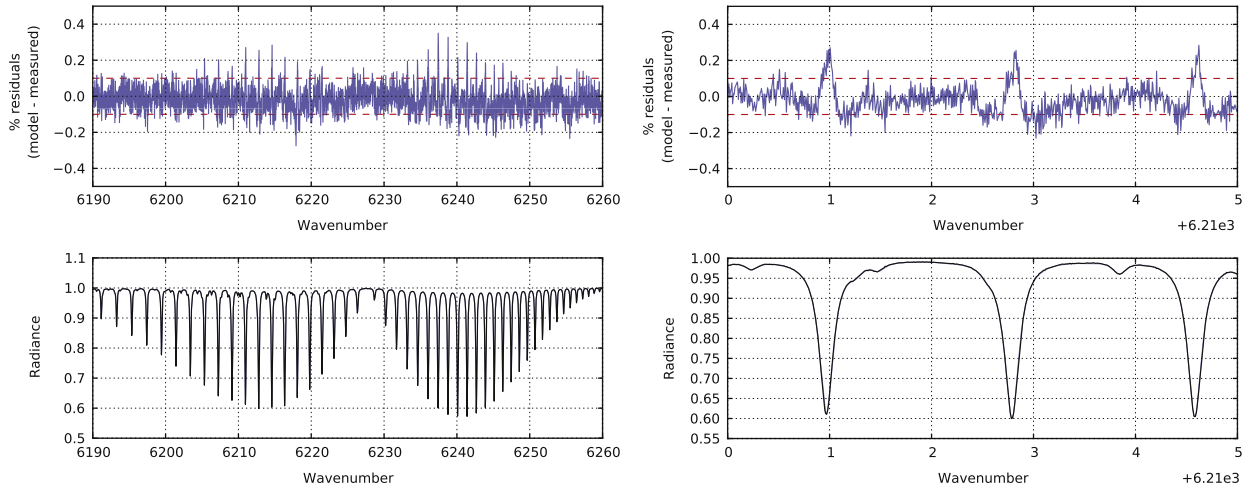

Fig. 2. Modeling an air-broadened CO_2 laboratory spectrum at 1.61 μm (wavenumber=cm^{-1}) by applying line parameters for a Speed Dependent profile with Line Mixing from [23,30]. The right plot shows an expanded view at 6212.5 cm^{-1}, and the red dashed lines mark the 0.1% radiometric accuracy target. Spectral resolution: 0.00667 cm^{-1} (optical path difference 75.0 cm); Optical path length: 32.54 m; Total gas pressure: 742.1 Torr at 295.3 K with 9.03% being ^{12}C-enriched $^{16}O^{12}C^{16}O$. (For interpretation of the references to color in this figure caption, the reader is referred to the web version of this article.)

solar path. Each station tracks the sun across a range of airmasses and seasons. These instruments have important advantages for our evaluation. Their high spectral resolution of 0.014 cm^{-1} is a stringent test of line shape subtleties. Their SNR is approximately 5000, an order of magnitude better than OCO-2. Viewing the solar disk center directly allows them to neglect atmospheric scattering effects, and the atmospheric conditions are constrained by sensors at the surface and occasional aircraft column measurements. They are true atmospheric measurements and observe phenomena that it is not feasible to measure in the lab experiments.

Here we evaluate performance on upward-looking atmospheric FTS spectra from a TCCON site in Park Falls, Wisconsin. We choose an initial dataset of 140 spectra from 22 December 2004 that has already been used in previous spectroscopic studies [25]. The soundings comprise a diverse dataset with varying SNR and airmasses ranging from less than 3 to over 12. Conditions at the ground site were very cold (−20 °C) and dry; this minimizes confounding effects

such as H_2O broadening of CO_2 and drawdown from photosynthesis. The measured surface pressure ranged from 964 hPa to 967 hPa, with a standard deviation of just 0.7 hPa. It is likely that $\mathbf{X}_{CO_2}$ did not change significantly during the day.

The upward-looking retrievals use a variant of the OCO-2 Level 2 algorithm with an *a priori* atmospheric model based on pressure and temperature profiles for that locale and day from the National Centers for Environmental Prediction (NCEP). These data are re-gridded into 70 atmospheric levels. A raytracing algorithm uses an oblate spheroid globe model to compute the path distance through each layer. It feeds into a radiative transfer code by Spurr [47] which performs computations of direct beam attenuation and refractive effects to simulate the observed spectrum. The retrieval rescales the entire vertical *a priori* abundance profile by a single scalar value that is treated as a free parameter. One can use this scaling factor, along with air pressure and water vapor abundances, to estimate the dry air column averaged mixing ratio of CO_2. Separate profile scaling factors are retrieved simultaneously for CH_4 and H_2O concentrations and atmospheric temperature. The retrieval fits these scalar parameters and the linear continuum to the measured spectrum. We also account for solar lines in this region. Our CO_2 absorption calculation uses the pre-computed cross sections without any online modifications to the individual line parameters or mixing.

We have found that isotopologue abundances in atmospheric retrievals have a slight but consistent offset from the laboratory-derived values. As compensation, we assume abundance ratios with an additional 6% enhancement of the $^{16}O^{12}C^{18}O$ isotopologue relative to the HITRAN standard. This is an expedient compromise since the computational constraints of OCO-2 retrievals prevent fitting each isotopologue's abundance independently at runtime. The 6% enhancement has proven consistent across multiple soundings and path lengths.

During a combined retrieval with both the 1.61 μm and 2.06 μm CO_2 bands, any disagreement in band strengths can preclude convergence to an optimal fit because the two bands work against each other producing different values of $\mathbf{X}_{CO_2}$. Consequently the total absorption cross sections of the two bands are scaled for mutual consistency and agreement with *a priori* atmospheric predictions from EMCWF profiles. This results in a further scaling factor of 0.99388 applied to the 2.06 μm band and 1.00539 to the 1.61 μm band.

We compare the proposed spectroscopic database against a benchmark standard from Lamouroux et al. [28]. The Lamouroux et al. [28] database differs in two ways: it uses a standard Voigt line shape, and computes LM using an alternative parametric form of the relaxation matrix. This parametric form is based on the Energy Corrected Sudden (ECS) model [48]. The ECS model relates all off-diagonal terms through a power law with four temperature- and perturber-dependent free parameters. A subsequent renormalization procedure guarantees consistency of the final result with detailed balance and the known diagonal elements. This contrasts with the proposed OCO-2 approach that uses nearest neighbor line mixing. Both databases use internally self-consistent parameters retrieved using the appropriate line shape assumptions. However we emphasize that the source data, line shape, and relaxation matrices all differ between the two alternatives so this comparison cannot attribute performance differences to a particular model choice. Instead, our test aims to characterize the empirical performance of these two state-of-the-art databases on atmospheric data. We will subsequently refer to the two methods as the *benchmark* and *proposed* approaches. We use these two alternative methods to compute cross sections for the P and R branches of the 1.61 μm and 2.06 μm bands. Isotopologue corrections are held constant between the two test scenarios, as are all other bands and absorbers.

Fig. 3 shows the residual of a typical 2.06 μm band sounding at 10 airmasses, shown as a percentage of

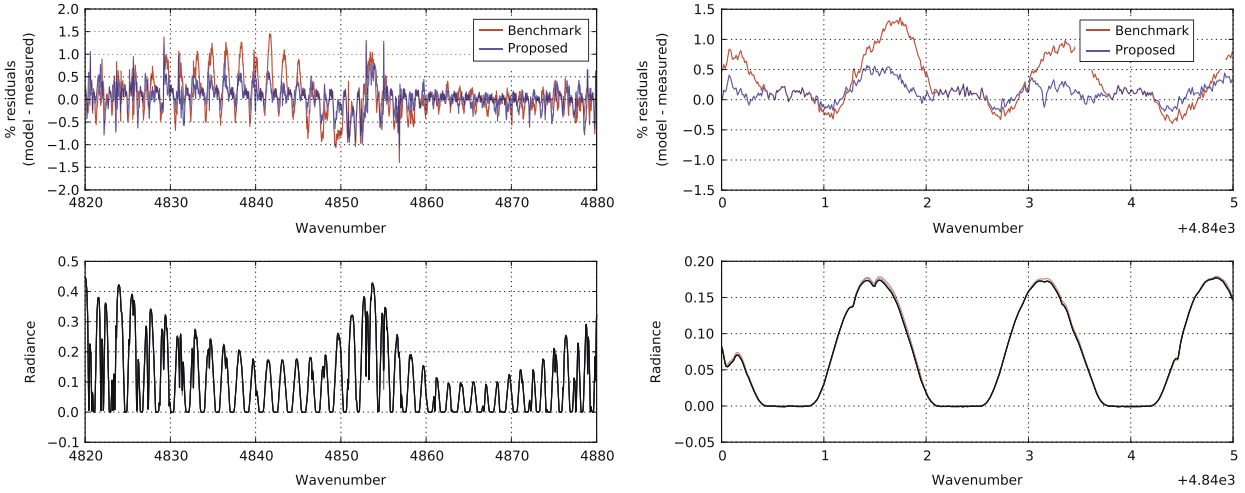

Fig. 3. Modeling a 10 airmass atmospheric spectrum at 2.06 μm. The spectrum is a ground-based sounding recorded at 0.014 cm^{-1} resolution with the TCCON Park Falls FTS station, 22 December 2004. The residuals in red are from the benchmark Line Mixing software and line list from Lamouroux et al. [28], while the residuals in blue are for the present proposed software and database (applied in Fig. 1) from Benner et al. [30] which combines a speed dependent profile and tridiagonal line mixing. (For interpretation of the references to color in this figure caption, the reader is referred to the web version of this article.)

maximum radiance. The red residual line shows the fit from the benchmark database, with structured residuals apparent in the P branch near 4840 cm^{-1} as noted in [25]. The proposed database improves this region. Several H_2O line residuals also appear; these are more difficult to address in this retrieval process due to differences between the actual column and the *a priori* atmospheric profile of H_2O mixing ratios. Fig. 4 shows a similar comparison of the 1.61 μm band. Here LM is less prominent, and performance improvements from the proposed database are more ambiguous.

Fig. 5 plots spectral residuals and $\mathbf{X}_{CO_2}$ for retrievals that use each band alone as well as a two band retrieval that fits both spectra simultaneously. The proposed database consistently improves the overall spectrum fit. The improvements are largest in the 2.06 μm band. Fig. 5 (Right) shows the retrieved $\mathbf{X}_{CO_2}$. Table 2 quantifies the airmass bias with the linear slope and correlation coefficients, and the Spearman ρ rank correlation coefficient for $\mathbf{X}_{CO_2}$ vs. airmass. The airmass bias improves somewhat (i.e. the slope magnitude is reduced) for each band taken alone as well as for the 2-band retrieval. Again, the largest benefit is for retrievals involving the 2.06 μm band.

3.2. Orbital retrievals with GOSAT

Prior to the OCO-2 launch, the team has worked directly with GOSAT data to refine the retrieval approach, and has benefited from partnership and generous support of the GOSAT and TANSO-FTS teams. The TANSO-FTS instrument offers 0.2 cm^{-1} spectral sampling, with resolution generally comparable to OCO-2. The GOSAT soundings introduce challenges of true space-based reflected sunlight measurements including pathlength uncertainties associated with scattering aerosols and the surface. Here we validate the new absorption cross sections using a selected sample of satellite data. Specifically, we provide

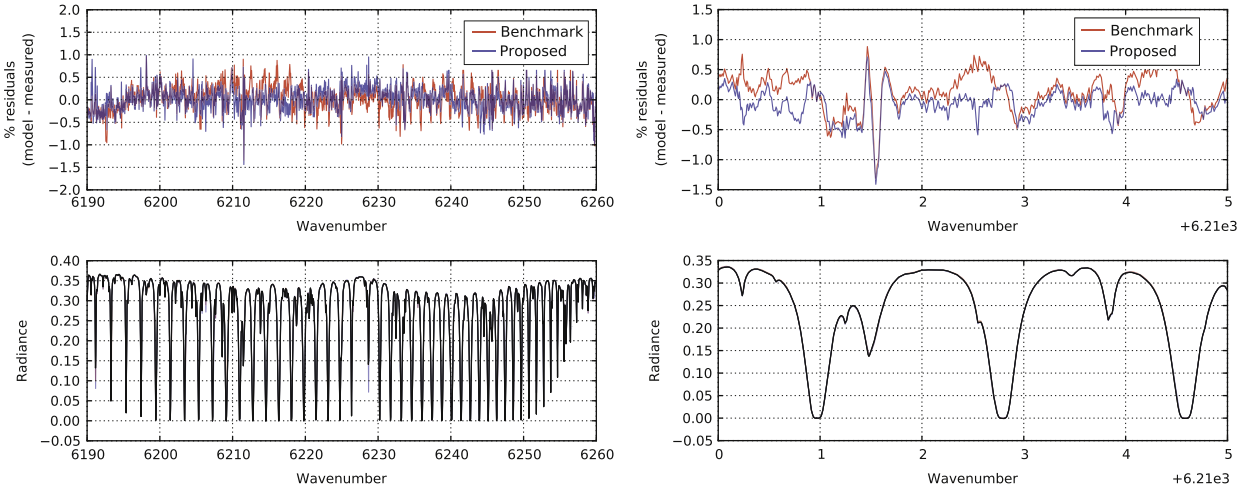

Fig. 4. TCCON spectral residual for a typical 10 airmass sounding in the 1.61 μm band from the Park Falls FTS station, 22 December 2004. The right panel shows detail of the fit at 6212.5 cm^{-1} (see text and Figs. 2 and 3).

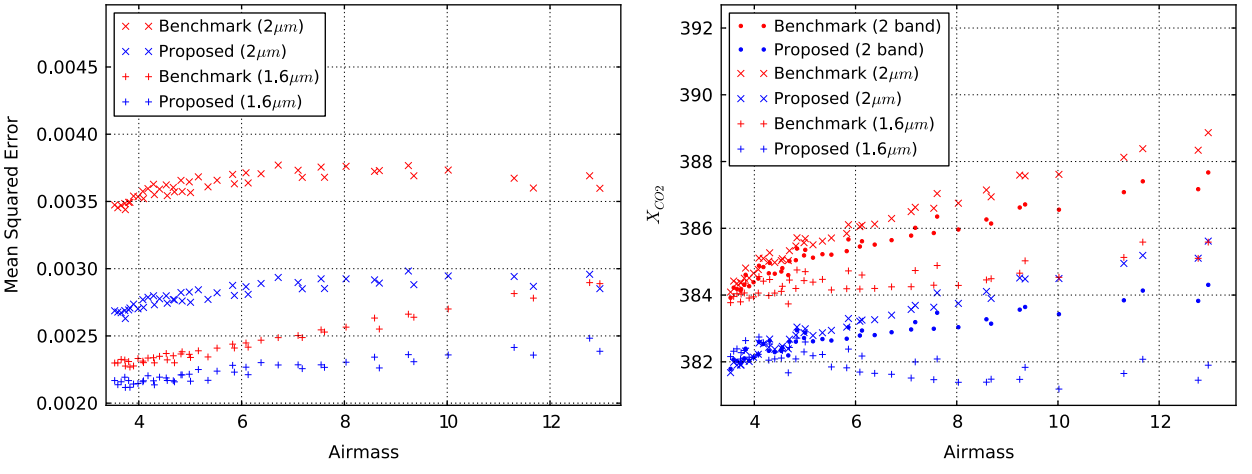

Fig. 5. Performance comparison of the two spectroscopic databases on a TCCON dataset from Park Falls, Wisconsin, 22 December 2004. Left: Mean squared relative error of the modeled and measured spectra. Right: retrieved $\mathbf{X}_{CO_2}$ as a function of airmass.

Table 2
Park Falls 22 December 2004 – retrieved $\mathbf{X}_{CO_2}$ values vs. airmass, comparing the reference benchmark and proposed line lists.

Result	**Both bands**		**2.06** μm		**1.61** μm	
	Benchmark	**Proposed**	**Benchmark**	**Proposed**	**Benchmark**	**Proposed**
Slope	0.355	0.219	0.468	0.376	0.131	−0.101
Corr	0.966	0.941	0.978	0.978	0.972	−0.651
ρ	0.980	0.962	0.987	0.983	0.738	−0.692

Table 3
Parameter sources used for the oxygen A band in GOSAT retrievals.

Parameter	**0.76** μm O_2
Positions	Robichaud [49,50]
Intensities	Robichaud [49,50] (see text)
Air-widths	Robichaud [49]
Air-shifts	Robichaud [49] (see text)
Air-width T dependence	Brown [52]
Line shapes	Voigt with Line Mixing
Isotopologues	Rothman [45]
Air LM	Tran [29]
Speed dependence	n/a
Continuum	CIA via Tran [29]
Collisional narrowing	n/a

retrieval results from a larger dataset consist of GOSAT soundings coincident with the TCCON ground stations, amounting to 425 spectra from orbits spanning multiple years, continents, and latitudes. These tests utilize the three-band OCO-2 algorithm which performs a simultaneous retrieval using both 1.61 μm and 2.06 μm regions.

The O_2 spectroscopy is held constant in this experiment but we provide details here for completeness (Table 3). Our O_2 absorption line parameters are based on the 2008 HITRAN database detailed by Rothman et al. [45]. Robichaud et al. [49,50] provide line positions and pressure-induced shifts, line intensities, air broadening and self-broadening parameters. One exception between ABSCO line parameters and those of the HITRAN 2008 are the strong lines of the R branch, for which custom pressure-induced shifts were provided by coauthor Brown. We use O_2 LM coefficients from the calculations referenced in [29]. Collisional narrowing parameters are available, but are not used. The OCO-2 retrieval algorithm currently exhibits a systematic air pressure error of approximately 10 hPa [12]. This is likely related to O_2 spectroscopy though retrieval or instrument effects may also play a role. As in [51,12], we rescale cross sections by a compensatory factor of 1.025 to remove the mean air pressure bias. This factor was derived from a larger representative dataset and applied to all retrievals in this comparison.

Fig. 6 shows the mean spectral residual, e.g. the average error combining all soundings. The 2.06 μm band generally corroborates the TCCON result. Fig. 7 shows that improvements at 1.61 μm are more ambiguous. Fig. 8 compares the goodness of fit scores from each sounding. This plot shows reduced χ^2 values associated with both bands of the three-band retrieval. The database with a speed dependent profile and new LM yields the largest reduction in mean χ^2 value for the 2.06 μm band, which drops from 1.09 to 1.00. The change in 1.61 μm is consistent but the magnitude is much smaller. Dark lines show the ratio χ^2 score produced by the proposed parameters as a fraction of the benchmark score on the same sounding. We plot this distribution on the same axis but with horizontal values interpreted as a fractional ratio. The proposed parameters reduce the χ^2 values in the 1.61 μm band by about 8% with respect to the benchmark. In the 2.06 μm band, the proposed parameters reduce χ^2 by 11% with respect to the benchmark.

Finally we compare these GOSAT retrievals to coincident retrievals by the TCCON network. Here we use the daily mean value from the TCCON retrieval algorithm, called GFIT [34], as a reference standard. As noted previously, an upward-looking estimate is intrinsically more accurate than the GOSAT result. Moreover, the GFIT TCCON retrievals have been extensively validated against in situ profiles provided by aircraft. It is not a perfect ground truth measurement since diurnal X_{CO_2} variation would cause the GOSAT estimate to deviate from the TCCON daily mean even if both retrievals were perfect. The algorithms also share some potential sources of bias, such as their *a priori* atmospheric profiles. Despite these caveats, a separate retrieval algorithm is a valuable check on the orbital $\mathbf{X}_{CO_2}$ accuracies.

We correct each $\mathbf{X}_{CO_2}$ result by a constant factor to zero out mean bias against TCCON observations. Finally, we apply standard filtering rules from the OCO-2 Level 2 algorithm. These rules, detailed by Crisp et al. [12], are a series of exclusion criteria based on retrieval values such as χ^2, retrieved aerosol optical depth and surface pressure. These filters exclude data that is contaminated by clouds or other intermittent retrieval failures.

Fig. 9 plots the GOSAT retrievals against the TCCON standard using each of the spectroscopic databases. Table 4 quantifies the agreement. The overall yield (number of soundings passing the filter rules) increases by 5%, while the average scatter (absolute difference against the TCCON values) decreases from 1.5 to 1.39 ppm. A slight improvement in the linear correlation score is not significant for this dataset size. Overall however these performance scores are consistent with a slight comparative advantage to the new database.

4. Discussion

Benchmark results broadly agree with previous analysis of the TCCON dataset that finds persistent structured residuals in the 2.06 μm band [25]. The proposed model parameters further improve the spectrum fit, showing consistent benefits for multiple instruments and retrieval methods. These tests span a range of path length,

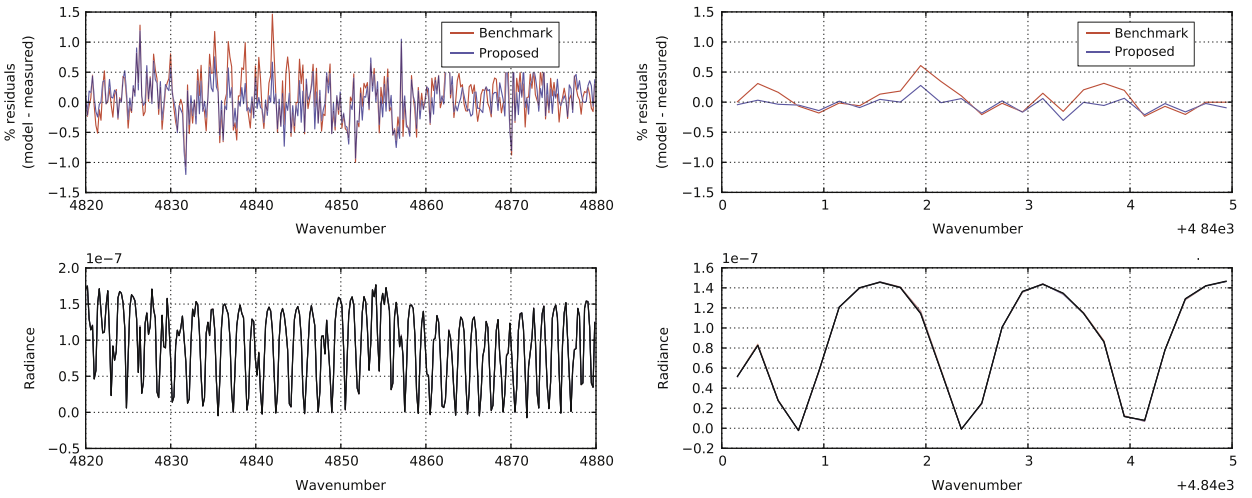

Fig. 6. Mean residuals in the 2.06 μm band for 425 GOSAT soundings covering a wide range of latitudes. As in Fig. 3, we compare the benchmark database of Lamouroux et al. [28] against the multispectrum retrieval of Benner et al. [30] using Speed Dependence with tridiagonal Line Mixing. The right panel shows a detailed view of the same mean residual.

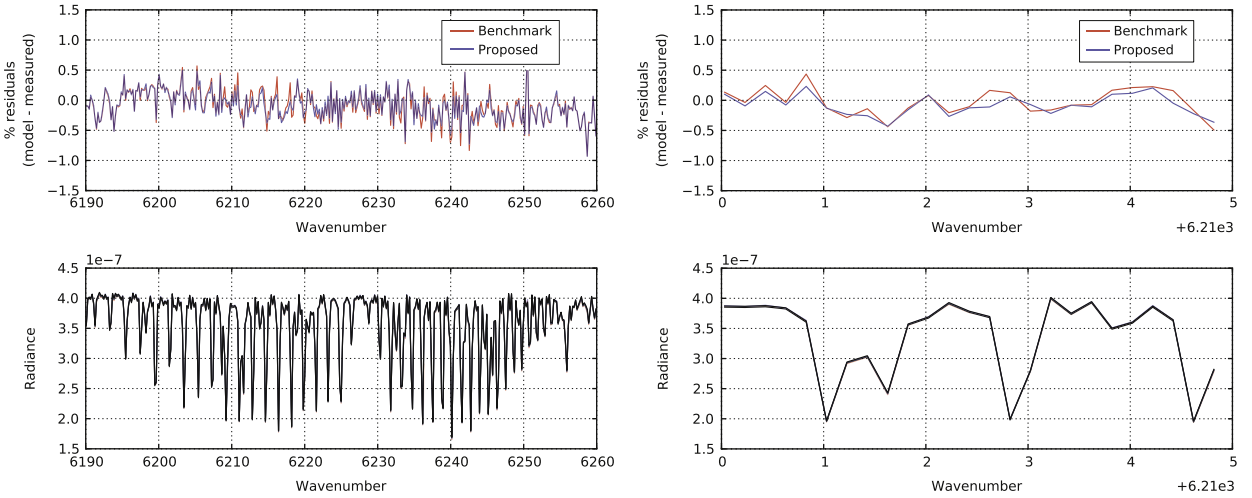

Fig. 7. Spectral residuals, similar to Fig. 6 but for the 1.61 μm region. The retrieval itself used all three OCO-2 bands.

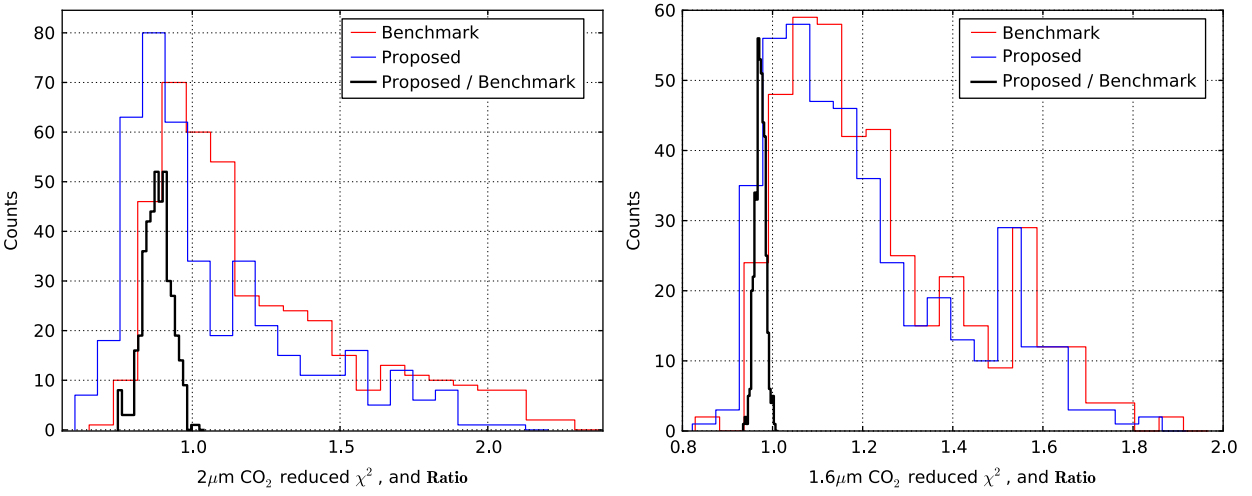

Fig. 8. Spectral residuals, showing the χ^2 values for both bands of the three-band retrieval. The mean χ^2 value drops from 1.09 to 1.00 in the 2.06 μm band after moving to the proposed database with a speed dependent line profile and tridiagonal mixing. The mean χ^2 also drops in the 1.61 μm band but the change is not as significant. Dark lines show the ratio of error scores (specifically, each sounding's χ^2 using the proposed parameters as a fraction of the sounding's χ^2 score using the benchmark parameters). These are plotted on the same axis, but horizontal values are interpreted as a fractional ratio. The mean ratio in the 1.61 μm band is 0.972 ($\sigma = 0.011$), and the ratio in the 2.06 μm band is 0.882 ($\sigma = 0.047$). The improvement is significant in both bands.

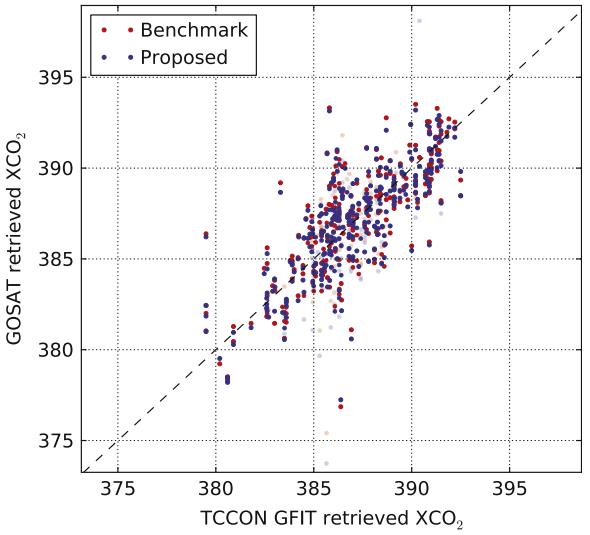

Fig. 9. Comparison of $\mathbf{X}_{CO_2}$ retrievals from the GOSAT satellite with estimates by the Total Column Carbon Observing Network (TCCON).

Table 4
Comparison of GOSAT soundings against coincident TCCON mean daily $\mathbf{X}_{CO_2}$ observations.

Result	**Benchmark**	**Proposed**
Successful retrievals	279 (65.6%)	300 (70.6%)
$\mathbf{X}_{CO_2}$ scatter	1.50 ppm	1.39 ppm
Correlation	0.767	0.781

temperature, and atmospheric conditions as well as different instrumental effects like saturation level, spectral resolution, and signal to noise ratios. The new database reduces spectral residuals while improving χ^2 goodness-of-fit. It increases the OCO-2 algorithm retrieval yield, and improves agreement with third-party $\mathbf{X}_{CO_2}$ estimates from a network of ground stations. On average, the new GOSAT retrieval predictions differ by 0.234 ppm which is a meaningful portion of the OCO-2 error budget. Such tests favor the new database over the alternatives currently available. Consequently the changes described here have been incorporated into the standard OCO-2 processing pipeline, where they have produced similar improvements in converged χ^2 goodness of fit values. Ultimately sub-percent retrieval accuracy for remote sensing demands significant refinement of existing spectroscopy, to which non-Voigt line shapes are a first step.

Despite these improvements the model does not fully achieve OCO-2 spectroscopic goals. First, systematic structures remain in 2.06 μm band retrievals at the 0.5% level, beyond desired accuracy limits. These structures could be related to unmodeled effects such as Dicke narrowing, temperature dependence of line mixing, or sources of continuum absorption not included here. The multispectrum fits used to derive line parameters do not yet resolve such phenomena. An asymmetric structure at the band center could be related to broad continuum-level effects, but its lack of alignment with known CIA continua [28] may be more consistent with line shape or line mixing inaccuracies. Such spectroscopic residuals may contribute to an airmass dependence that remains even under the best atmospheric retrieval conditions (e.g. TCCON data collected on dry days). The "glint" mode of OCO-2 will enable high-SNR retrievals with very high airmasses, magnifying any airmass dependence in CO_2 spectroscopy.

The spectral fit improvements described here have done little to ameliorate this airmass dependence, which is consistent with other bottlenecks in the $\mathbf{X}_{CO_2}$ estimate beyond CO_2 line shape. Other contributors may include the solar spectrum model, atmospheric profile differences from the ECMWF prior, path-dependent differences in isotopic fractionation, and continuum-level absorption due to dimers or interferences. We cannot exclude these other effects, nor can we ignore line shape inaccuracies while systematic residuals remain.

5. Conclusions

We describe a direct retrieval of tridiagonal relaxation matrix elements and line shape parameters simultaneously, which significantly reduces the structured residuals seen at atmospheric optical depths. The best fits use a speed dependent line shape, which is consistent with laboratory results.

While our comparison cannot conclusively attribute performance to a specific physical model or line shape, it underscores the influence of line shapes and line mixing parameterization on the retrieval. For OCO-2, attention to these factors is crucial to achieve the 1 ppm accuracies needed to identify sources and sinks on a global scale. The TCCON network of FTIR spectrometers provides invaluable validation because its high SNR and spectral resolution observations can use long optical path lengths to achieve a large range of opacities. Atmospheric spectra from both ground-based (upward-looking) and orbiting (downward-looking) sensors can validate the spectroscopy required for OCO-2 glint observations, provided the same molecular line profiles are applied in all cases.

The tests described here have implications for spectroscopic remote sensing in general. The atmospheric community has begun to employ some non-Voigt line shapes, such as the speed dependent Voigt for H_2O [53]. It has also considered line mixing for CO_2 [25]. It is generally acknowledged that reaching sub-1% accuracies in atmospheric retrievals will require substantially improved laboratory results [54]. Future progress depends on correct understanding of molecular line shapes and having a consistent set of accurate line parameters.

Acknowledgments

We thank the OCO-2 ACOS Level 2 algorithm team including Annmarie Eldering, Vivienne Payne and Michael Gunson. We thank the members of the OCO-2 science team including Eli Mlawer and Iouli Gordon. We have also benefited from the counsel of Mitchio Okumura, Joseph Hodges, and David Long. GOSAT TANSO-FTS spectra were provided to the ACOS Team through a GOSAT Research Announcement (RA) agreement between the California

Institute of Technology and the three parties, JAXA, NIES and the MOE. The European Centre for Medium-Range Weather Forecasts (ECMWF) provided meteorological data for initializing the retrievals. The Total Carbon Column Observing Network (TCCON) Archive, operated by the California Institute of Technology, supplied upward-looking measurements. U.S. funding for the Park Falls TCCON station comes from NASA's Terrestrial Ecology Program, grant number NNX11AG01G. A portion of the research described was carried out at the Jet Propulsion Laboratory, California Institute of Technology and The College of William and Mary under contracts with the National Aeronautics and Space Administration.

References

[1] Chevallier F, Fisher M, Peylin P, Serrar S, Bousquet P, Breon FM, et al. Inferring CO_2 sources and sinks from satellite observations: method and application to TOVS data. J Geophys Res 2005;110:D24309.
[2] Ciais P, Rayner P, Chevallier F, Bousquet P, Logan M, Peylin P, et al. Atmospheric inversions for estimating CO_2 fluxes: methods and perspectives. Clim Change 2010;103:69–92.
[3] Chevallier F, Deutscher NM, Conway TJ, Ciais P, Ciattaglia L, Dohe S, et al. Global CO_2 fluxes inferred from surface air-sample measurements and from TCCON retrievals of the CO_2 total column. Geophys Res Lett 2011;38:L24810.
[4] Miller C, Crisp D, DeCola PL, Olsen SC, Randerson JT, Michalak AM, et al. Precision requirements for space-based XCO_2 data. J Geophys Res 2007;112:D10314, http://dx.doi.org/10.1029/2006JD007659.
[5] Chevallier F, Breon FM, Rayner PJ. Contribution of the orbiting carbon observatory to the estimation of CO_2 sources and sinks: theoretical study in a variational data assimilation framework. J Geophys Res 2007;112:D09307.
[6] Rayner PJ, OBrien DM. The utility of remotely sensed CO_2 concentration data in surface source inversions. Geophys Res Lett 2001;28:175–8.
[7] Gurney KR, Law RM, Denning AS, Rayner PJ, Baker D, Bousquet P, et al. Towards robust regional estimates of CO_2 sources and sinks using atmospheric transport models. Nature 2002;415:626–30.
[8] OBrien DM, Rayner PJ. Global observations of the carbon budget. 2. CO_2 column from differential absorption of reflected sunlight in the 1.61 μm band of CO_2. J Geophys Res 2002;107:4354, http://dx.doi.org/10.1029/2001JD000617.
[9] Crisp D, Atlas RM, Breon FM, Brown LR, Burrows JP, Ciais P, et al. The Orbiting Carbon Observatory (OCO) mission. Adv Space Res 2004;34:700–9.
[10] Crisp D, Miller CE, DeCola PL. NASA Orbiting Carbon Observatory: measuring the column averaged carbon dioxide mole fraction from space. J Appl Rem Sens 2008. http://dx.doi.org/10.1117/1.2898457.
[11] Boesch H, Baker D, Connor B, Crisp D, Miller CE. Global characterization of CO_2 column retrievals from shortwave-infrared satellite observations of the Orbiting Carbon Observatory-2 mission. Remote Sens 2011;3:270–304.
[12] Crisp D, Fischer BM, Dell O'C, Frankenberg C, Basilio R, Boesch H, et al. The ACOS XCO_2 retrieval algorithm, Part II. Global XCO_2 data characterization. Atmos Meas Tech Discus 2011;4:1–59.
[13] Reuter M, Bovensmann H, Buchwitz M, Burrows JP, Connor BJ, Deutscher NM, et al. Retrieval of atmospheric CO_2 with enhanced accuracy and precision from SCIAMACHY: validation with FTS measurements and comparison with model results. J Geophys Res 2011;116:D04301.
[14] Hamazaki T, Kaneko Y, Kuze A, Kondo K. Fourier transform spectrometer for greenhouse gases observing satellite (GOSAT). Proc SPIE 2005;5659:73.
[15] Yokota T, Yoshida Y, Eguchi N, Ota Y, Tanaka T, Watanabe H, et al. Global concentrations of CO_2 and CH_4 retrieved from GOSAT: first preliminary results. SOLA Sci Online Lett Atmos 2009;5:160–3.
[16] Dell O'CW, Connor B, Bösch H, O'Brien D, Frankenberg C, Castano R, et al. The ACOS CO_2 retrieval algorithm Part 1: description and validation against synthetic observations. Atmos Meas Tech Discus 2011;4:6097–158, http://dx.doi.org/10.5194/amtd-4-6097-2011.
[17] Rodgers C. Inverse methods for atmospheric sounding: theory and practice. Singapore: World Scientific; 2000.
[18] Miller CE, Brown LR, Toth RA, Benner DC, Devi VM. Spectroscopic challenges for high accuracy retrievals of atmospheric CO_2 and the Orbiting Carbon Observatory (OCO) experiment. Comp Rend Phys 2005;6:876–87.
[19] Chevallier F. Impact of correlated observation errors on inverted CO_2 surface fluxes from OCO measurements. Geophys Res Lett 2007;34:L24804.
[20] Washenfelder RA, Toon GC, Blavier JFL, Yang Z, Allen NT, Wennberg PO, et al. Carbon dioxide column abundances at the Wisconsin Tall Tower site. J Geophys Res 2006;111:D22305, http://dx.doi.org/10.1029/2006JD007154.
[21] Wunch D, Toon G, Blavier J, Washenfelder R, Notholt J, Connor B, et al. The Total Carbon Column Observing Network. Philos Trans R Soc A 2011;369:2087.
[22] Brault JW, Brown LR, Chackerian Jr. C, Freedman R, Predoi-Cross A, Pine AS. Self-broadened CO line shapes in the v=2-0 band. J Mol Spectrosc 2003;222:220–39.
[23] Devi VM, Benner DC, Brown LR, Miller CE, Toth RA. Line mixing and speed dependence in CO_2 at 6227.9 cm^{-1}: constrained multispectrum analysis of intensities and line shapes in the 30013 ← 00001 band. J Mol Spectrosc 2007;245:52–80.
[24] Long DA, Bielska K, Lisak D, Havey DK, Okumura M, Miller CE, et al. The air-broadenedbb near-infrared CO_2 line shape in the spectrally isolated regime: evidence of simultaneous Dicke narrowing and speed dependence. J Chem Phys 2011;135:064308.
[25] Hartmann JM, Tran H, Toon GC. Influence of line mixing on the retrievals of atmospheric CO_2 from spectra in the 1.6 and 2.1 μm regions. Atmos Chem Phys 2009;9:7303–12, http://dx.doi.org/10.5194/acp-9-7303-2009.
[26] Strow LL, Hannon SE, Souza-Machado SD, Motteler HE, Tobin D. An overview of the AIRS radiative transfer model. IEEE Trans Geosci Rem Sens 2003;41:303–13.
[27] Niro F, Hase F, Camy-Peyret C, Payan S, Hartmann JM. Spectra calculations in central and wing regions of CO_2 IR bands between 10 and 20 μm II atmospheric solar occultation spectra. J Quant Spectrosc Radiat Transfer 2005;90:43–59.
[28] Lamouroux J, Tran H, Laraia AL, Gamache RR, Rothman LS, Gordon IE, et al. Updated database plus software for line-mixing in CO_2 infrared spectra and their test using laboratory spectra in the 1.5−2.3 μm region. J Quant Spectrosc Radiat Transfer 2010;111:2321–31.
[29] Tran H, Hartmann JM. An improved O_2 A band absorption model and its consequences for retrievals of photon paths and surface pressures. J Geophys Res 2008;113:1–11.
[30] Benner DC, Devi VM, Nugent E, Sung K, Brown LR, Miller CE. et al., Line parameters of carbon dioxide in the 4850 cm^{-1} region. In: Twenty-second Coll on High resolution molecular spectroscopy, Dijon, Fr 2011; poster N19, in preparation.
[31] Predoi-Cross A, Liu W, Holladay C, Unni AV, Schofield I, McKellar ARW, et al. Line shape parameters measurement and computations for self-broadened carbon dioxide transitions in the 30012←00001 and 30013←00001 bands, line mixing, and speed dependence. J Mol Spectrosc 2007;245:34–51.
[32] Boone CD, Walker KA, Bernath PF. Speed-dependent Voigt profile for water vapor in infrared remote sensing applications. J Quant Spectrosc Radiat Transfer 2007;105:525–32.
[33] Vitcu A. Line shape studies in the 0310-0110 Q branch of N_2O using a mid-infrared difference-frequency spectrometer. PhD dissertation, University of Toronto; 2003.
[34] Wunch D, Toon G, Wennberg P, Wofsy S, Stephens B, Fischer M, et al. Calibration of the total carbon column observing network using aircraft profile data. Atmos Meas Tech 2010;3:1351–62.
[35] Benner DC, Rinsland CP, Devi VM, Smith MAH, Atkins D. A mulitspectrum nonlinear least squares fitting technique. J Quant Spectrosc Radiat Transfer 1995;53:705–21.
[36] Hartmann J, Boulet C, Robert D. Collisional effects on molecular spectra: laboratory experiments and models, consequences for applications. Amsterdam: Elsevier; 2008.
[37] Predoi-Cross A, Unni AV, Heung H, Devi VM, Benner DC, Brown LR. Line mixing effects in the v_2+v_3 band of methane. J Mol Spectrosc 2007;246:65–76.
[38] Levy A, Lacome N, Chackerian Jr. C. Collisional line mixing, vol. 1. Boston: Academic Press; 1992. p. 261–337.
[39] Pine AS. Line mixing sum rules for the analysis of multiplet spectra. J Quant Spectrosc Radiat Transfer 1997;57:145–55.
[40] Rodrigues R, Boulet C, Bonamy L, Hartmann JM. Temperature pressure and perturber dependencies of line-mixing effects in

CO_2 infrared spectra. II. Rotational angular momentum relaxation and spectral shift in $\Sigma \leftarrow \Sigma$ bands. J Chem Phys 1998;109:3037–47.
[41] Priem D, Rohart F, Colmont JM, Wlodarczak G, Bouanich JP. Lineshape study of the $J = 3 \leftarrow 2$ rotational transition of CO perturbed by N_2 and O_2. J Mol Struct 2000;517:435–54.
[42] Pine AS, Ciurylo R. Multispectrum fits of Ar-broadened HF with a generalized asymmetric lineshape: effects of correlation, hardness, speed dependence, and collision duration. J Mol Spectrosc 2001;208:180–7.
[43] Predoi-Cross A, McKellar ARW, Benner DC, Devi VM, Gamache RR, Miller CE, et al. Temperature dependences for air-broadened Lorentz half-width and pressure shift coefficients in the $30013 \leftarrow 00001$ and $30012 \leftarrow 00001$ bands of CO_2 near 1600 nm. Can J Phys 2009;87:517–35.
[44] Toth RA, Brown LR, Miller CE, Devi VM, Benner DC. Spectroscopic database of CO_2 line parameters: 4300–7000 cm^{-1}. J Quant Spectrosc Radiat Transfer 2008;109:906–21.
[45] Rothman LE, Gordon IE, Barbe A, Benner DC, Bernath PF, Birk M, et al. HITRAN 2008 molecular spectroscopic database. J Quant Spectrosc Radiat Transfer 2009;110:533–72.
[46] Sung K, Brown LR, Toth RA, Crawford TJ. FT-IR measurements of H_2O-broadened half-widths of CO_2 at 43 μm. Can J Phys 2009;87:469–84.
[47] Spurr R. Code for Direct Beam Attenuation.Jet Propulsion Laboratory, California Institute of Technology, Personal Communication via Vijay Natraj; 2011.
[48] Niro F, Boulet C, Hartmann JM. Spectra calculations in central and wing regions of CO_2 IR bands between 10 and 20 μm. I: Model and laboratory measurements. J Quant Spectrosc Radiat Transfer 2004;88:483–98.
[49] Robichaud DJ, Hodges JT, Brown LR, Lisak D, Maslowski P, Yeung LY, et al. Experimental intensity and lineshape parameters of the oxygen A-band using frequency-stabilized cavity ring-down spectroscopy. J Mol Spectrosc 2008;248:1–13.
[50] Robichaud DJ, Hodges JT, Maslowski P, Yeung LY, Okumura M, Miller CE, et al. High-accuracy transition frequencies for the O_2 A-band. J Mol Spectrosc 2008;251:27–37.
[51] Butz A, Guerlet S, Hasekamp O, Schepers D, Galli A, Aben I, et al. Toward accurate CO_2 and CH_4 observations from GOSAT. Geophys Res Lett 2011;38:L14812.
[52] Brown LR, Plymate C. Experimental line parameters of the oxygen A band at 760 nm. J Mol Spectrosc 2000;199:166–79.
[53] Schneider M, Hase F, Blavier JF, Toon GC, Leblanc T. An empirical study on the importance of a speed-dependent voigt line shape model for tropospheric water vapor profile remote sensing. J Quant Spectrosc Radiat Transfer 2010;112:465–74.
[54] Harrison JJ, Bernath PF, Kirchengast G. Spectroscopic requirements for accurate, a microwave and infrared-laser occultation satellite mission. J Quant Spectrosc Radiat Transfer 2011;112:2347–54.